

See discussions, stats, and author profiles for this publication at: <https://www.researchgate.net/publication/231400289>

Hydrogen fluoride/hydrogen chloride vibrational and rotational distributions from three- and four-centered unimolecular elimination reactions

ARTICLE *in* THE JOURNAL OF PHYSICAL CHEMISTRY · FEBRUARY 1991

Impact Factor: 2.78 · DOI: 10.1021/j100157a008

CITATIONS

43

READS

16

3 AUTHORS, INCLUDING:



Elangannan Arunan

Indian Institute of Science

104 PUBLICATIONS 1,797 CITATIONS

SEE PROFILE



Sanjay Wategaonkar

Tata Institute of Fundamental Research

72 PUBLICATIONS 948 CITATIONS

SEE PROFILE

ARTICLES

HF/HCl Vibrational and Rotational Distributions from Three- and Four-Centered Unimolecular Elimination Reactions

E. Arunan, S. J. Wategaonkar, and D. W. Setser*

Department of Chemistry, Kansas State University, Manhattan, Kansas 66506 (Received: June 26, 1990; In Final Form: September 17, 1990)

The infrared chemiluminescence from the HF elimination reactions of CF_3H , CF_3CH_3 , $\text{C}_2\text{H}_5\text{F}$, $\text{C}_2\text{F}_5\text{H}$, $n\text{-C}_3\text{F}_7\text{H}$, and $i\text{-C}_3\text{F}_7\text{H}$ has been used to assign the vibrational and rotational distributions of HF. The chemically activated fluoroalkane molecules were formed by H atom recombination with the appropriate fluoroalkyl radicals, which were generated by reactions of H atoms with the fluoroalkyl iodide precursor molecules. The HF vibrational distributions decline monotonically with increasing energy. The mean HF vibrational energy is larger than the statistical expectation, and 25–35% of the potential energy of the exit channel is specifically released as HF vibrational energy. The $\text{HF}(v)$ rotational excitation is modest, and $\langle E_R(\text{HF}) \rangle$ seems to be equal to or less than the statistical expectation. The $\text{HF}(v, J)$ distributions are used to discuss the dynamics of these HF elimination reactions. The energy disposal pattern from the HF elimination reaction from CF_3H is compared to the vibrational energy distributions of HCl from the CF_2HCl , CFH_2Cl , and CFHCl_2 molecules that were generated by secondary reactions in the $\text{F} + \text{CFH}_2\text{Cl}$, CH_3Cl , and CH_2Cl_2 systems. In general, three-centered reactions of halomethanes release a larger fraction of the potential energy as $\langle E_V(\text{HX}) \rangle$ than do four-centered reactions of haloethanes.

Introduction

There is considerable current interest in the dynamics of the unimolecular HF and HCl elimination reactions from haloalkanes. Potential surfaces have been developed to evaluate the dynamics for the four-centered process,^{1–3} and there is a need for improved experimental data for the product energy distributions for comparison with theory. The lifetimes of molecules for both the three- and four-centered processes at energies of $\sim 100 \text{ kcal mol}^{-1}$ are consistent with RRKM statistical predictions. Therefore, a statistical energy distribution is assured at the transition-state configuration. In this work we have used infrared chemiluminescence (IRCL) from HF or HCl to study the energy disposal from elimination reactions that release a significant amount of potential energy in the exit channel. All the three-centered reactions occur on singlet potential surfaces to yield singlet carbenes. Our goal is to better understand how the potential energy in the exit channel is released to the products.

The vibrational and translational energy disposal from HF and HCl elimination reactions has been studied by several techniques; however, little information exists with regard to the rotational distributions.^{4–9} Several studies have utilized the photoactivation of haloethylenes, the prevailing viewpoint being that internal conversion is rapid and the HX elimination occurs on the ground-state potential.^{5,8} Recent experiments with fluoroalkanes have utilized multiphoton IR-laser pumping with observation of

HF or HCl vibrational energy⁷ or the translational energy release.¹⁰ The complete CF_2 energy distribution from HCl elimination¹¹ of CF_2HCl and the CHF vibrational energy from HCl elimination¹² of CFH_2Cl have been reported. The vibrational energy in the olefin fragment from four-center elimination has been assigned by chemical activation methods.¹³

Zamir and Levine¹⁴ (hereafter referred to as ZL) provided a survey for the vibrational and translational energy disposal for elimination reactions in 1980 and interpreted the results by information theoretic analysis. The $\langle f_V(\text{HX}) \rangle$ is in near accord with the prior distribution for most of the three-centered reactions, as would be expected because the potential energy released in the exit channel is small. The λ_V values from the linear surprisal plots for the four-centered reactions show that more than the statistical amount of energy is released to $E_V(\text{HX})$. ZL developed a constraint by treating the excess energy and the potential energy in the exit channel as a sum rule to characterize both translational and vibrational distributions. However, Leone's group⁸ and Sloan's group⁹ have used a variable HF frequency, based on expectations about the transition state, to calculate vibrational distributions that matched their experimental observations. They view the $\text{HF}(v)$ distribution as statistical, but the phase space available for HF is decided early in the exit channel, where the HF stretching frequency is lower than in the asymptotic limit. Our interpretations will emphasize the statistical partitioning of the excess energy, $E_X = \langle E \rangle - E_0$, at the transition state followed by a specific release of the potential energy, E_P , as the system traverses the exit channel.^{1,13,14}

There is little knowledge about HF or HCl rotational energy distributions. Fletcher and Leone⁸ assigned a temperature of approximately 15000 K to the $\text{HF}(v)$ rotational distribution arising from photoelimination of CH_2CFCl . Quick and Wittig⁷ fitted

- (1) Kato, S.; Morokuma, K. *J. Chem. Phys.* **1980**, *73*, 3900.
- (2) Benito, R. M.; Santamaria, J. *J. Phys. Chem.* **1988**, *92*, 5028.
- (3) Raff, L. M.; Graham, R. W. *J. Phys. Chem.* **1988**, *92*, 5111.
- (4) (a) Chang, H. W.; Setser, D. W.; Perona, M. J. *J. Phys. Chem.* **1971**, *75*, 2070. (b) Manocha, A. S.; Setser, D. W.; Wickramartchi, M. A. *Chem. Phys.* **1983**, *76*, 129. The $\text{HCl}(v)$ distribution from HCFCl_2 is reported here.
- (5) Clough, P. N.; Polanyi, J. C.; Taguchi, R. T. *Can. J. Chem.* **1970**, *48*, 2919.
- (6) (a) Sirkin, E. R.; Berry, M. J. *IEEE J. Quantum Electron.* **1974**, *QE-10*, 701. (b) Berry, M. J. In *Molecular Energy Transfer*; Levine, R., Jortner, J., Eds.; Wiley: New York, 1976; p 114. P_1/P_0 values of 0.8 ± 0.2 and 0.6 ± 0.1 from $\text{CH}_2\text{F} + \text{CH}_3$ and $\text{H} + \text{CH}_2\text{CH}_2\text{F}$, respectively, are quoted. We used an average value of 0.7.
- (7) Quick, Jr., C. R.; Wittig, C. *J. Chem. Phys.* **1980**, *72*, 1694.
- (8) Fletcher, T. R.; Leone, S. R. *J. Chem. Phys.* **1988**, *88*, 4720.
- (9) (a) Donaldson, D. J.; Watson, D. G.; Sloan, J. J. *Chem. Phys.* **1982**, *68*, 95. (b) Donaldson, D. J.; Sloan, J. J. *J. Chem. Phys.* **1985**, *82*, 1873. (c) Sloan, J. J. *J. Phys. Chem.* **1988**, *92*, 18.

- (10) Sudbo, A. S.; Schultz, P. A.; Shen, Y. R.; Lee, Y. T. *J. Chem. Phys.* **1978**, *69*, 2312.
- (11) Stephenson, J. C.; King, D. S. *J. Chem. Phys.* **1978**, *69*, 1485.
- (12) Samsonov, Yu. N.; Petrov, A. K. *Chem. Phys. Lett.* **1981**, *84*, 183.
- (13) (a) Holmes, B. E.; Setser, D. W.; Pritchard, G. O. *Int. J. Chem. Kinet.* **1976**, *8*, 215. (b) Holmes, B. E.; Setser, D. W. *J. Phys. Chem.* **1978**, *82*, 2450, 2461. (c) Holmes, B. E.; Setser, D. W. In *Physical Chemistry of Fast Reactions*; Smith, I. W. M., Ed.; Plenum: New York, 1980; Vol. 2, p 83.
- (14) Zamir, E.; Levine, R. D. *Chem. Phys.* **1980**, *52*, 253.

TABLE I: Thermochemistry of the Three-Centered Elimination Reactions^a

reactant	$\langle E \rangle$	ΔH°_0	E_0	$\langle E \rangle - \Delta H^\circ_0^b$	E_P^c	E_X^d
CF ₃ H	108.6 ± 1.8	56.2 ± 2.5	71.0 ± 3.8	52.4 ± 2.5	14.8 ± 3.8	37.6 ± 3.8
CF ₂ HCl	115.0 ± 5.0 ^e	48.0 ± 4.6	56.0 ± 3.8	67.0 ± 5.0	~8.0 ^f	59.4 ± 5.5
CFH ₂ Cl	111.5 ± 4.1	64.8 ± 6.1	73.3 ± 6.1	46.7 ± 6.1	~8.5 ^f	38.2 ± 6.1
CFHCl ₂	112.0 ± 4.2	42.4 ± 7.0	51.3 ± 4.0	69.6 ± 7.0	~8.9 ^f	60.7 ± 6.1

^aSee Figure 1 for definitions of symbols; all values are in kcal mol⁻¹. The entries pertain to HF elimination for CF₃H and HCl elimination for the other molecules. ^bTotal available energy for the products. ^cThe potential energy barrier, $E_0 - \Delta H^\circ_0$, for the reverse reaction. ^dExcess energy for reaction, $\langle E \rangle - E_0$, which is statistically distributed to the internal degrees of freedom at the transition-state geometry. ^eUsing $\Delta H^\circ_f(\text{CFHCl})$ from ref 21 gives $\langle E \rangle = 121 \pm 6$. We prefer the lower estimate. ^fThese E_P values are not well established. The formal uncertainty in E_P should be the sum of the uncertainties in ΔH°_0 and E_0 ; these uncertainties are larger than E_P . The very large value for $E_0(\text{CFH}_2\text{Cl})$ is suspect, but it is consistent with $\Delta H^\circ_f(\text{CFH})$; see refs 22 and 12.

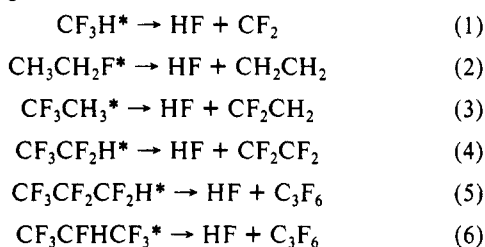
TABLE II: Thermochemistry of the Four-Centered Elimination Reactions^a

reactant	$\langle E \rangle$	ΔH°_0	E_0	$\langle E \rangle - \Delta H^\circ_0^b$	E_P^c	E_X^d
CH ₃ CH ₂ F	100.0 ± 3.0 ^e	9.0 ± 1.0	58.0 ± 1.0	91.0 ± 3.0	49.0 ± 2.0	42.0 ± 3.0
CF ₃ CH ₃	109.6 ± 2.0	30.8 ± 2.5	68.0 ± 2.0	78.8 ± 2.5	37.2 ± 2.5	41.6 ± 2.5
CF ₃ CF ₂ H	106.3 ± 1.0	39.4 ± 2.5	68.0 ± 2.0	66.9 ± 2.5	28.6 ± 2.5	38.3 ± 2.5
<i>n</i> -C ₃ F ₇ H	106 ± 2.0	28 ± 10	68 ± 2	78 ± 10	~40	~38
<i>i</i> -C ₃ F ₇ H	105 ± 2.0	28 ± 10	67 ± 2	77 ± 10	~39	~38

^aSee Figure 1 for definitions of symbols; all values are in kcal mol⁻¹. All entries pertain to four-centered HF elimination. ^bTotal available energy for the products. ^cThe potential energy barrier, $E_0 - \Delta H^\circ_0$, for the reverse reaction. ^dExcess energy for reaction, $\langle E \rangle - E_0$, which is statistically distributed to the internal degrees of freedom at the transition-state configuration. ^eThe β C-H bond energy is not available, but it is expected to be higher than the α C-H bond energy, which is 97.3 kcal mol⁻¹ (ref 21b). ^fSince the $\Delta H^\circ_f(i\text{-C}_3\text{F}_7\text{H})$ is not well established, the $\Delta H^\circ_f(n\text{-C}_3\text{F}_7\text{H})$ was used; the C-H bond energy at 298 K of *i*-C₃F₇H is known.

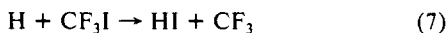
their low-resolution HF emission spectra from IRMPD experiments of fluorinated ethanes with rotational temperatures of 800–1000 K. Stephenson and King reported the rotational distribution of CF₂ from the IRMPD of CF₂HCl, CF₂Br₂, and CF₂Cl₂.¹¹

In the present work we have used IRCL from a fast flow reactor to measure the vibrational and rotational energy disposal to HF for the following reactions:



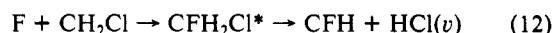
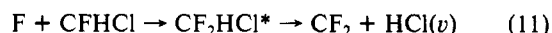
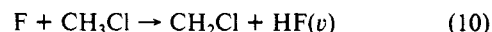
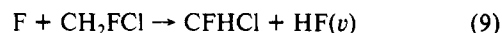
Besides nascent HF(*v*) vibrational distributions, partially arrested rotational distributions can be observed in our flow reactor,¹⁵ if the reaction generates HF(*v*,*J*) states above $J \approx 8$. The present study refines the existing HF(*v*) distributions for reactions 2 and 3 and provides new information for the other reactions. The rotational excitation is largest for CF₃H, followed by CF₃CH₃, C₂F₃H, and CH₃CH₂F. The observed HF(*v*) rotational distributions were 300 K Boltzmann for the C₃F₇H reactions. The $\langle J_R(\text{HF}) \rangle$ was found to be close to the statistical limit, and the elimination reactions do not generate large amounts of HF rotational energy. In general, the HX(*v*) distributions from elimination reactions decline monotonically with increasing *v* and have $\langle J_v(\text{HX}) \rangle$ values of ~0.15, which contrasts strongly with the inverted distributions from the abstraction reactions of H by F atoms.^{15c} Although the $\langle E_v(\text{HX}) \rangle$ and $\langle E_R(\text{HX}) \rangle$ from elimination reactions are modest, the distributions still provide insight into the reaction dynamics.

The activated molecules were generated in 0.5 Torr of Ar carrier gas by H atom addition to the radical, which had been created by abstraction of I from a stable precursor, e.g.



The secondary reactions are fast enough that the unimolecular elimination products following reactions 1–6 can be observed. The rate constant¹⁶ for reaction 7 is 1.4×10^{-11} cm³ s⁻¹, and that¹⁷ for reaction 8 is 8.9×10^{-11} cm³ s⁻¹. Rate constants for the other abstraction and recombination reactions are expected to be similar. Iodine atom abstraction is the dominant primary channel rather than F abstraction or H substitution for reaction 7.¹⁶ The Einstein coefficient for HI is so small that IRCL from HI formed by abstraction reactions could not be observed, even for long periods of signal averaging.

The HCl elimination reactions from CF₂HCl and CFH₂Cl were included in this investigation because the energy disposal to CF₂ and CFH is known and adding the HCl energy distribution can give a complete picture. Changing HF to HCl is unlikely to seriously affect the dynamics, and the HCl elimination data should complement the CF₃H reaction. The CFHCl₂ reaction has been previously studied,^{4b} and those data will be included. The activated molecules were formed by secondary recombination of CFHCl and CH₂Cl radicals with F as shown in eqs 9–12. Rotational



relaxation of HCl in Ar is faster than for HF, and we only observed 300 K Boltzmann distributions for the HCl(*v*) molecules. Unlike the H atom reactions with RI, the above primary reactions give strong HF(*v*) primary emission. The HF(*v*) distribution from reaction 9 is first reported here.

Tables I and II summarize the thermochemistry for these reactions; the energy terms are defined in Figure 1. The average energies, $\langle E \rangle$, of the molecules in reactions 1–6, 11, and 12 were determined from the sum of the ΔH°_0 for the recombination reaction, the thermal energy of the reactants, and an assumed activation energy of 1 kcal mol⁻¹. The following ΔH°_f (in kcal mol⁻¹) were used in computing the values listed in Tables I and II: H (51.6), HF (-65.1), HCl (-22.0), CF₂ (-43.6), CF₃ (-111.7), CF₃H (-164.9), C₂H₄ (52.5), C₂F₄ (-156.6), CF₂HCl (-113.6), CFH₂Cl (-60.8), and CFHCl₂ (-66.4);^{18a} CH₃CF₃

(15) (a) Wategaonkar, S. J.; Setser, D. W. *J. Chem. Phys.* **1989**, *90*, 251, 6223. (b) Wategaonkar, S. J.; Setser, D. W. *J. Chem. Phys.* **1987**, *86*, 4477. (c) Agrawalla, B.; Setser, D. W. In *Gas Phase Chemiluminescence and Chemi-ionization*; Fontijn, A., Ed.; Elsevier: Amsterdam, 1985.

(16) Morris, R. A.; Donohue, K.; McFadden, D. L. *J. Phys. Chem.* **1989**, *93*, 1358.

(17) Ryan, K. R.; Plumb, I. C. *Plasma Chem. Plasma Process.* **1984**, *1*, 141.

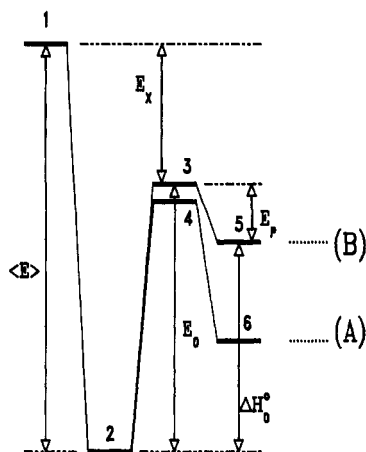


Figure 1. Schematic energy level diagram for (A) three- and (B) four-centered elimination reactions drawn to scale for CF_3H and CF_3CH_3 , respectively: (1) $\text{H} + \text{CF}_3/\text{CF}_3\text{CH}_3$, (2) $\text{CF}_3\text{H}/\text{CF}_3\text{CH}_3$, (3) three-centered transition state, (4) four-centered transition state, (5) $\text{CF}_2 + \text{HF}$, and (6) $\text{C}_2\text{F}_2\text{H}_2 + \text{HF}$. The thermochemical values for all reactions are summarized in Table I and II.

(-172.9) and CH_2CF_2 (-77.0);^{18b} CF_3CF_2 (-211.8), CF_3CH_2 (-123.6), and $\text{CF}_3\text{CF}_2\text{CF}_2$ (-310.5);¹⁹ $\text{CF}_3\text{CF}=\text{CF}_2$ (-275.3);²⁰ CHCl_2 (22.6), CH_2Cl (28.1), and CFHCl (-15.4);²¹ CFH (26.0) and CFCl (-2.0).²² The threshold energy, E_0 , for HF elimination of CF_3H ,²³ CF_3CH_3 ,²⁴ $\text{CH}_3\text{CH}_2\text{F}$,²⁴ and $\text{CF}_3\text{CF}_2\text{H}$ ²⁵ and for HCl elimination of CF_2HCl ²⁶ and CFHCl_2 ²⁷ were taken from the literature. The threshold energy for CFH_2Cl was calculated by using the ΔH_f° for the elimination reaction and the reverse activation barrier reported in the literature.¹² The threshold energy for the $\text{C}_3\text{F}_7\text{H}$ molecules was taken to be the same as $\text{CF}_3\text{CF}_2\text{H}$ following Kato et al.²⁵ The $\Delta H_f^\circ(\text{C}_3\text{F}_7)$ values are not well-known, and Benson's group additivity method was employed. Particularly for fluoro compounds this method can be in large error, sometimes by 10 kcal mol⁻¹ or even more. As will become evident, we believe that the three- and four-centered channels are both operative for $\text{CF}_3\text{CF}_2\text{H}$ and possibly also for $\text{C}_3\text{F}_7\text{H}$.

Experimental Methods

The experimental method is the same as for our recent work, except that the primary and secondary reactions both occur in the same linear flow reactor.¹⁵ The H or F atoms were generated by microwave discharge of H_2/Ar or CF_4/Ar mixtures, which were added at the front of the reactor. The Ar carrier gas was added separately at the entrance of the reactor. The reagent was added via a ring injector 20 cm downstream from the atom inlet as a 5–10% mixture in Ar just before the observation window (4-cm-diameter NaCl flat). Typical concentrations of H and the iodide reagent were $(1\text{--}3) \times 10^{13}$ and $(0.3\text{--}2.0) \times 10^{13}$ molecules cm⁻³, respectively. The H atom concentration was estimated by assuming 50% dissociation of the H_2 .^{15a} The CF_4 concentration was kept in the range $(1\text{--}10) \times 10^{12}$ molecules cm⁻³; 1–2 F atoms are generated per CF_4 molecule.

(18) (a) Chase, Jr., M. W.; Davies, C. A.; Downey, Jr., J. R.; Frurib, D. J.; Mcdonald, R. A.; Syverud, A. N. *J. Phys. Chem. Ref. Data* **1985**, *14*, (Suppl No. 1). (b) Wagman, D. D.; Evans, W. H.; Parker, V. B.; Schumm, R. H.; Halow, J.; Bailey, S. M.; Churney, K. C.; Nuttall, R. L. *J. Phys. Chem. Ref. Data* **1982**, *11* (Suppl. No. 2).

(19) Rodgers, A. S. *ACS Symp. Ser.* **1978**, No. 66, 296.

(20) Papina, T. S.; Kolesov, V. P.; Golovanova, Yu. G. *Zh. Fiz. Khim.* **1987**, *61*, 2233; *Chem. Abstr.* **1987**, *107*, 162949.

(21) (a) Tschuikow-Roux, E.; Paddison, S. *Int. J. Chem. Kinet.* **1987**, *19*, 15. (b) Tschuikow-Roux, E.; Salomon, D. R. *J. Phys. Chem.* **1987**, *91*, 699.

(22) Lias, S. G.; Karpas, Z.; Liebman, J. F. *J. Am. Chem. Soc.* **1985**, *107*, 6089.

(23) Schug, K. P.; Wagner, H. Gg.; Zabel, F. *Ber. Bunsen-Ges. Phys. Chem.* **1979**, *83*, 167.

(24) Chang, H. W.; Craig, N. L.; Setser, D. W. *J. Phys. Chem.* **1972**, *76*, 954.

(25) Kato, S.; Makide, Y.; Tominaga, T.; Takeuchi, K. *J. Phys. Chem.* **1987**, *91*, 4278.

(26) Oref, I.; Rabinovitch, B. S. *J. Phys. Chem.* **1977**, *81*, 2587.

(27) Sofer, I.; Yagov, A. *Chem. Phys. Lett.* **1988**, *149*, 439.

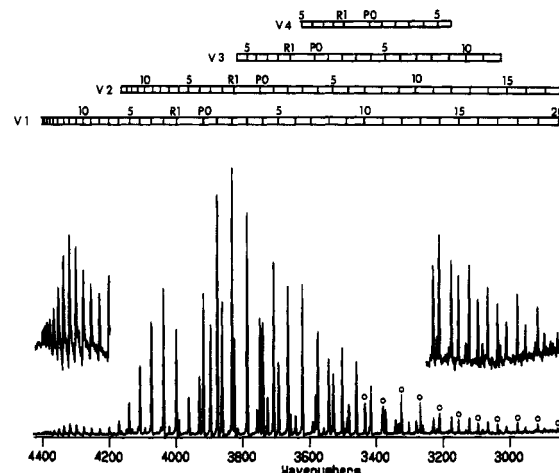


Figure 2. HF(v,J) emission spectrum from the CF_3H elimination reaction for $[\text{H}_2] = 2.0 \times 10^{13}$ and $[\text{CF}_3\text{I}] = 6.0 \times 10^{12}$ molecules cm⁻³. The rotational lines from $J \geq 10$ for HF($v=1$) are indicated.

TABLE III: Comparison of RRKM Rate Constants and Collision Frequency

reactant	energy, kcal mol ⁻¹	$k(\text{elim})$, s ⁻¹	Z , ^c 10 ⁶ s ⁻¹	ref
CF_3H	109	2.5×10^{11}	3.5	34
CF_2HCl	115	1.1×10^{12}	3.9	a, 26
CFH_2Cl	112	1.5×10^{11}	3.9	a
CFHCl_2	112	3.0×10^{12}	4.2	34
CF_3CH_3	109	8.2×10^8	4.7	24
$\text{CH}_3\text{CH}_2\text{F}$	100	2.8×10^9	3.7	1, 24
$\text{CF}_3\text{CF}_2\text{H}$	106	9.2×10^8	4.5	24
$n\text{-C}_3\text{F}_7\text{H}$	106	5.0×10^5	4.8	25
$i\text{-C}_3\text{F}_7\text{H}$	105	1.5×10^6	4.8	b

^a The same model as for CFHCl_2 (ref 34) was used to develop the frequencies for the transition state. Our transition states for three-centered elimination have preexponential factors of $(2\text{--}3) \times 10^{13}$ s⁻¹, in accord with recent experimental measurement of the Arrhenius constants.²³ ^b RRKM calculations are not available for $i\text{-C}_3\text{F}_7\text{H}$. The rate constant were assumed to be the same as for $n\text{-C}_3\text{F}_7\text{H}$ after adjusting for the 3-fold higher reaction path degeneracy. ^c 0.5 Torr of Ar.

The linear flow velocity was typically 120 m s⁻¹, corresponding to a reaction time of 0.2 ms for an observation length of about 2.5 cm. The Ar pressure could be varied from 0.3 to 1.0 Torr without loss of pumping speed. For these conditions the HF(v) and HCl(v) relaxation was fully arrested, and the rotational relaxation of HF was partly arrested. The $J = 0\text{--}6$ levels of HF(v) have a 300 K rotational distribution; but, the populations observed in $J \geq 8$ depend upon whether or not the reaction generates HF(v) in high- J states. It was necessary to increase the reaction time to ~ 1 ms for the HCl elimination reactions and for the HF elimination from $\text{C}_3\text{F}_7\text{H}$ in order to get a favorable signal-to-noise ratio. For these conditions the vibrational distributions of the primary HF(v) product from reactions 10 and 11 were modified to some extent. However, the vibrational distribution from the secondary reaction was less affected by relaxation and the observed distributions are close to the nascent ones, even for 1-ms reaction time. The observed rotational distributions were entirely 300 K Boltzmann for the HCl elimination reactions and for the $\text{C}_3\text{F}_7\text{H}$ reactions.

The emission spectra at 1–2-cm⁻¹ resolution were recorded with the Biorad (FTS-60) FTIR spectrometer; individual rotational lines are easily observed as shown in Figure 2. The rotational population in individual levels was obtained from the peak height of each line after division by the instrumental response function and the Einstein coefficient²⁸ for the particular transition.

Commercial tank grade Ar was purified by passage through molecular sieve traps cooled to liquid N₂ temperature. Tank grade

(28) Oba, D.; Agrawalla, B. S.; Setser, D. W. *J. Quant. Spectrosc. Radiat. Transfer* **1985**, *34*, 283.

TABLE IV: HF(ν) Distributions from Elimination Reactions^a

reagent	P_0	P_1	P_2	P_3	P_4	λ_ν	$\langle f_\nu \rangle^b$	ref
CF ₃ H	50.0	58.0	30.0	10.0	2.0	-5.1	0.16 (0.06)	this work
	50.0	30.0	14.4	5.0	1.0			31
CF ₃ CH ₃	43.0	53.0	32.0	12.0	3.0	-10.5	0.13 (0.02)	this work
	48.0	30.2	18.2	6.8	1.7			6
CH ₃ CH ₂ F ^d		33.7	18.3				0.12 ^c	5
		62.7	27.5	7.8	2.0			this work
CF ₃ CF ₂ H	37.2	41.1	31.1	18.9	6.9 ^d	-10.1	0.15 (0.03)	7
		25.6	19.4	11.8	4.3			this work
<i>n</i> -C ₃ F ₇ H ^e		50.0	30.0	12.5	7.5	-6.8	0.06 (0.02)	this work
	68.0	82.8	14.8	2.0	0.4			
<i>i</i> -C ₃ F ₇ H ^e		26.6	4.5	0.8		-14.1	0.06 (0.01)	this work
	66.9	73.3	20.0	6.7				
		24.2	6.6	2.3		-14.0	0.06 (0.01)	this work
	68.0	68.7	25.3	6.0				
		22.0	8.0	2.0				

^a The second line for each entry gives the renormalized results after assigning P_0 from either laser gain experiments or linear surprisal plot; see text. ^b Number in parentheses is the $\langle f_\nu \rangle$ calculated for the prior. ^c This is the $\langle f_\nu \rangle$ if P_0 is assigned from the laser gain measurement of P_0/P_1 . ^d This reaction also gives $\nu = 5$ with $P_5 = 2.0$, after assigning P_0 and renormalization $P_5 = 1.7$. ^e The reaction time for the C₃F₇H reactions was 1 ms, whereas the time was 0.2 ms for all other reactions.

H₂ was used without further purification. All reagents were purified by several freeze-pump-thaw cycles before loading. The CF₃I, C₂F₅I, CF₃CH₂I, CF₃CF₂I, and CF₃CF₂CF₂I were purchased from PCR Inc.; CH₂FCH₂I was obtained from Columbia Organic Chemicals Co. The CH₃Cl, CH₂FCl, and CF₄ were from standard sources.

Results

1. *General Considerations.* The molecules formed by H/F atom recombination have ~ 105 – 110 kcal mol⁻¹ of energy and can either undergo unimolecular reaction or be collisionally stabilized. In principle, the molecules can react in more than one way, i.e., HF/HCl elimination, C–C bond cleavage, or C–H/C–X bond cleavage. RRKM calculations show that in this energy range only HF or HCl elimination needs to be considered. The rate for C–C cleavage is orders of magnitude lower, and C–F and C–H bond rupture have even higher threshold energies and smaller rate constants. Table III lists the RRKM rate constants for HF/HCl elimination along with estimates of the collision frequency in Ar. Collisional stabilization is faster than unimolecular reaction rates for the C₃F₇H molecules. This was evident in our experiments as the HF signal from reactions 5 and 6 were 2 orders of magnitude weaker than from CF₃H and CF₃CH₃. Also, increasing the Ar pressure from 0.4 to 2.0 Torr reduced the HF emission intensity for the C₃F₇H* reactions. There may be a small contribution to the HF(ν , J) yield from C₃F₇H* molecules that have lost some energy through collisions with Ar. But, the unimolecular rate constants decline sharply with energy, and the majority of the observed HF(ν) is from C₃F₇H* molecules that have not experienced multiple collisions with Ar.

Before presenting the HX distributions, the nature of the elimination channels for reactions 1–6, 11, and 12 will be considered. Obviously, CF₃H has only a three-centered transition state. The HCl channel is dominant for CHF₂Cl and CH₂FCl because the threshold energy is lower than for HF elimination.^{10,29} The CH₃CH₂F and CH₃CF₃ reactions proceed by four-centered transition states. The possibility of both three- and four-centered processes must be considered for CF₃CF₂H because halogen substitution on the α -carbon lowers the threshold energy for three-centered elimination.^{13a} Tschuikow-Roux et al.^{30a} assumed four-centered HF elimination from CF₃CF₂H in their shock tube studies; however, three-centered elimination followed by F migration is possible.^{30b} The energy available to HF in a three-centered process would be much less than that for the four-centered elimination, because most of the potential energy is released as

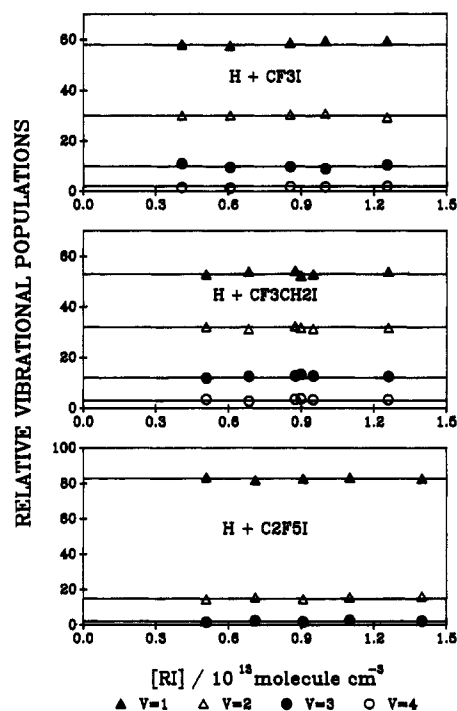


Figure 3. HF(ν) distribution as a function of [RI] for the H + CF₃I, C₂F₅I, and CF₃CH₂I systems. The [H₂] was typically 2.0×10^{13} molecules cm⁻³, the Ar pressure was 0.5 Torr, and the reaction time was 0.2 ms.

CF₃CF rearranges to C₂F₄. The thermochemistry given in Table II for CF₃CF₂H pertains to the four-centered elimination. The *i*- and *n*-C₃F₇H molecules could react by three- or four-centered pathways, and the HF(ν) distributions will be examined for evidence to distinguish between the two possibilities.

2. *Vibrational Distributions.* a. *HF Elimination Reactions.* The HF emission spectra were collected for a range of H and reagent concentrations. Figure 3 shows that the vibrational distributions from CF₃H, C₂F₅H, and CF₃CH₃ were independent of reagent concentration; the reaction time was 0.2 ms. The HF(ν) distributions also were invariant with [H], and we conclude that these are nascent distributions. The HF(ν) distributions from reactions 1–6 are summarized in Table IV. None of these HF(ν) distributions extended up to the thermochemical limit. Although $\nu = 4$ was observed from CF₃H, the available energy is sufficient to populate $\nu = 5$. The CF₃CH₃ reaction could give $\nu = 8$, but $\nu = 5$ was the highest observed level. The distributions from CH₃CH₂F and CF₃CF₂H extended to $\nu = 5$ and $\nu = 4$, but the thermochemistry allows $\nu = 9$ and 6, respectively.

(29) Martinez, R. I.; Herron, J. T. *Chem. Phys. Lett.* **1981**, *84*, 180.

(30) (a) Tschuikow-Roux, E.; Millward, G. E.; Quiring, W. J. *J. Phys. Chem.* **1971**, *75*, 3493. (b) Setser, D. W.; Lee, T. S.; Danen, W. C. *J. Phys. Chem.* **1985**, *89*, 5799.

TABLE V: HCl(v) Distributions from Elimination Reactions^a

reagent	P_0	P_1	P_2	P_3	P_4	λ_v	$\langle f_v \rangle^b$	ref
CF ₂ HCl		51.4	26.5	15.1	7.0			this work
	43.8	28.9	14.9	8.5	3.9	-2.2	0.12 (0.09)	
CFH ₂ Cl		59.2	25.3	9.9	5.6			this work
	43.9	34.0	14.7	5.1	2.3	-3.5	0.15 (0.08)	
CFHCl ₂ ^c		47.0	23.0	18.0	8.0			4b
	37.2	29.5	14.4	11.3	5.0	-3.2	0.14 (0.09)	

^aThe second line for each entry gives the results based upon assignment of P_0 from a linear surprisal plot. These experiments required a reaction time of 1 ms, and these results are lower limits to the nascent distributions; see text. ^bNumber in parentheses gives the $\langle f_v \rangle$ calculated for the prior.

^cThis reaction also gives $P_5 = 4.0$; after including P_0 and renormalization, $P_5 = 2.6$.

The IRCL experiments cannot give the population in $v = 0$, but our results can be combined with laser gain measurements, which usually obtain the P_0 to P_1 ratio, to assign P_0 for the CF₃H, CF₃CH₃, and CH₃CH₂F reactions. For other reactions, P_0 was obtained from the intercept of a linear surprisal plot. The model for the prior included all degrees of freedom of the HF and polyatomic product without angular momentum constraint to the calculation of the density of states.^{13c}

Bittenson reported the $v = 0, 1$, and 2 populations for CF₃H elimination using laser gain measurements,³¹ and our P_1/P_2 ratio agrees with his value. This prompts us to base our P_0 on his P_0/P_1 ratio (1.67). The distribution from reaction 1 fits a linear surprisal with $\lambda_v = -5.1$. Surprisal analysis of just our P_1 - P_4 data gives $P_0 = 0.39$ and $\lambda_v = -5.5$. The $\langle f_v \rangle$ of the observed distribution is 0.16 as opposed for the prior distribution.

Quick and Wittig⁷ reported the HF(v) distribution (P_1 - $P_4 = 50:30:12.5:7.5$) from IRMPD excitation of CH₃CH₂F. Our distribution extends to somewhat higher vibrational energy, as would be expected for our larger $\langle E \rangle$. Berry^{6b} reported only the P_0/P_1 ratio, 1.5, for this reaction. A surprisal calculation for our P_1 - P_5 data closely reproduces this P_0 value. The $\langle f_v \rangle$ is 0.15 with $\lambda_v = -10.1$; $\langle f_v \rangle$ is only 0.03 for the prior distribution. These f_v and λ_v values are typical for elimination reactions from haloethanes.¹⁴

Our HF(v) distribution for CF₃CH₃ differs slightly from Clough et al.'s⁵ results, who used the CF₃ + CH₃ reaction for activation ($\langle E \rangle = 99$ kcal mol⁻¹). Sirkin and Berry⁶ used H + CH₂CF₃ and CF₃ + CH₃ reactions to form CF₃CH₃ and obtained the $v = 0, 1$, and 2 population from laser gain measurements; both activation reactions gave the same HF(v) distribution. Our P_1/P_2 ratio is in reasonable agreement with Sirkin and Berry's value, and their P_0/P_1 ratio was used to obtain the P_0 value. The P_0 assigned by linear surprisal extrapolation from our P_1 - P_4 distribution matches this P_0 . The $\langle f_v(\text{HF}) \rangle$ is 0.13; the prior distribution gives $\langle f_v(\text{HF}) \rangle = 0.02$.

The vibrational distributions from the C₂F₅H and C₃F₇H reactions have not been previously reported; therefore, the $v = 0$ populations were assigned from linear surprisal plots. The C₂F₅H reaction gave the coldest HF(v) distribution; $\langle f_v \rangle$ is 0.06 and λ_v is -6.8, which is 2-fold smaller than for CF₃CH₃ or C₂H₅F. This is interpreted as evidence for a three-centered component to this reaction.

For the *i*- and *n*-C₃F₇H reactions the observation time had to be increased to 1 ms, and there may have been a small degree of HF(v) vibrational relaxation. For example, under these conditions the HF(v) distribution for the CF₃H reaction was P_1 - $P_4 = 63:29:7:1$ rather than 58:30:10:2. This comparison shows that the observed HF(v) distributions should still closely approximate the nascent distributions. The HF(v) distributions from both *i*- and *n*-C₃F₇H are nearly the same and extend only to $v = 3$. The $\langle f_v \rangle$ of 0.06 ($\lambda_v = -14$) is 6 times larger than the $\langle f_v \rangle$ for a prior distribution that includes all degrees of freedom. The P_2 and P_3 values are higher than that for the C₂F₅H reaction, which may indicate a greater relative importance of the three-centered pathway for the latter. The HF(v) distributions from the C₃F₇H reactions should be treated with some caution; the weak emission intensity, the possibility of modification of the C₃F₇H* energy

by Ar collisions, and the uncertain thermochemistry make the $\langle f_v(\text{HF}) \rangle$ assignment somewhat uncertain. Although the distributions from C₃F₇H are more extended than for C₂F₅H, the $\langle E \rangle$ also is larger and all have $\langle f_v(\text{HF}) \rangle = 0.06$.

b. HCl Elimination Reactions. The rate constant, 2.2×10^{-11} cm³ s⁻¹, for reaction 10^{15c} is comparable to the primary steps for the H atom reactions, but the rate constant for reaction 9^{4b} is only about 0.54×10^{-11} cm³ s⁻¹. The HF(v) distribution observed for 0.2-ms reaction time from F + CH₃Cl was P_1 : P_2 : $P_3 = 6:35:59$, which agrees with earlier reports.^{15c} The HF(v) distributions from CH₂FCI, P_1 : P_2 : $P_3 = 4:34:62$, was also sharply peaked at $v = 3$. The Einstein coefficient for HCl($v=1$) is roughly 1/5 that of HF($v=1$), and in order to observe the HCl emission from the secondary reaction, the observation time had to be increased to ~ 1 ms. For these operating conditions the HF emission intensity was about 2 orders of magnitude stronger than from HCl. The product of Ar pressure and reaction time was $(0.8-1.2) \times 10^{-3}$ Torr-s, whereas it was 0.2×10^{-3} Torr-s for reactions 1-4. The HF(v) distributions from the primary reactions were altered under these conditions, and P_1 - P_4 was 21:32:45:2 from F + CH₃Cl. In addition to HF($v=4$), emission from higher rotational levels of HF($v=1,2$) than in the nascent HF(v) distribution was observed. The majority of the HF(v) relaxation was from $v \rightarrow R, T$ relaxation by collisions with the reagent or F atoms. However, there may have been minor contributions to HF(v) formation from HF elimination (from CH₂FCI*), and the observation of HF($v=4$) suggests a small degree of energy pooling by HF(v). No attempt was made to deconvolute these effects, as our interest was in the HCl(v) distributions.

Table V lists the HCl(v) distributions from CF₂HCl, CFH₂Cl, and CFHCl₂. The degree of vibrational relaxation of HCl(v) should be less than for HF(v) from the primary reaction for two reasons. Firstly, the HCl($v=1,2$) relaxation rate constants with CH₃Cl probably are smaller than for HF($v=3$).³² Secondly, the HCl(v) is formed later in the reaction sequence and experiences fewer collisions. Several experiments were done with the 1-ms time for a range of [F] and [RCl], but there was no significant change in the HCl(v) distributions. The very minor difference in the HF(v) distribution from H + CF₃ mentioned earlier for the 1-ms reaction time vs the 0.2-ms time also should be remembered. Nevertheless, the HCl(v) distributions are quoted as lower estimates to the nascent distributions. Linear surprisal plots were used to estimate the P_0 values. We also examined Boltzmann plots for this purpose. Although the Boltzmann plots were linear, the P_0 values were larger than for the linear surprisal extrapolation. Considering the good agreement between the surprisal extrapolation and the experimental P_0 values for the HF elimination reactions, we decided in favor of the lower P_0 values. The $\langle f_v(\text{HCl}) \rangle$ are 0.12, 0.15, and 0.14 with $\lambda_v = -2.2, -3.5$, and -3.2 for CF₂HCl, CFH₂Cl, and CFHCl₂, respectively. These $\langle f_v \rangle$ values are 1.3-1.9 times higher than for the prior distribution. The slightly lower λ_v values for these HCl elimination reactions vs the CF₃H reaction may be a consequence of smaller E_p . However, the E_p values for these three reactions are not well-known, because of the uncertainty in the ΔH_f° of the carbenes, and detailed comparison between the results in Table V is not justified. Nevertheless, the HCl(v) distributions resemble the

(31) Bittenson, S. N. Ph.D. Thesis, University of Wisconsin, Madison, WI 1977.

(32) (a) Raybone, D.; Wategaonkar, S. J.; Setser, D. W. *J. Chem. Phys.* **1988**, *89*, 3384. (b) Leone, S. R. *J. Phys. Chem. Ref. Data* **1982**, *11*, 953.

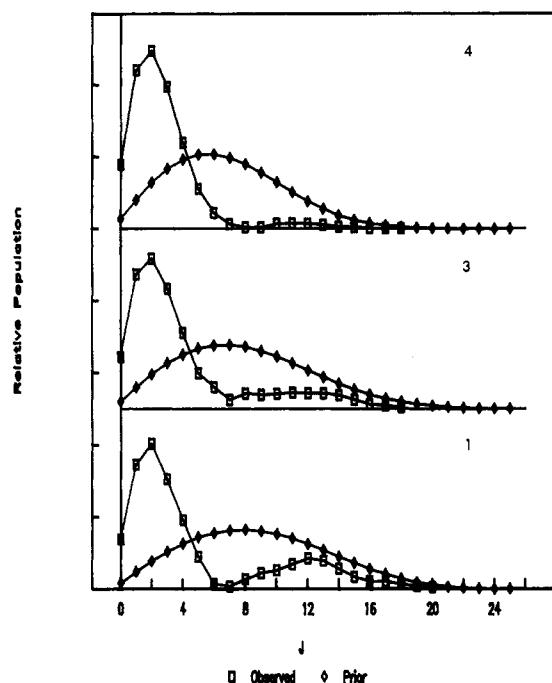


Figure 4. HF($v=1$) rotational distributions for reactions 1, 3, and 4 obtained for 0.5-Torr operating conditions. The rotational distributions calculated from the priors (with all degrees of freedom included) are shown for comparison.

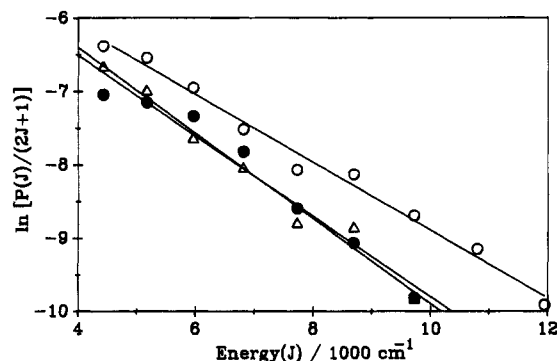


Figure 5. Boltzmann temperature assignments to the HF($v=1$) rotational populations with $J \geq 12$ from the CF₃H (O), CF₃CH₃ (●), and C₂F₅H (Δ) reactions.

HF(v) distribution from CF₃H, and the dynamics of the three-centered elimination is largely unaffected by changing HF to HCl.

3. HF(v) Rotational Distributions. In order to record the least relaxed distributions, experiments were done for the shortest time and the lowest Ar pressure for which optimum pumping speed could be maintained. For the best conditions the product of the Ar pressure and the observation time ($P\Delta t$) was 1.0×10^{-4} Torr·s. The rotational relaxation from HF(v) levels above $J \approx 8$ are partly arrested, but populations in $J \leq 7$ are 300 K Boltzmann. Figure 4 shows the HF($v=1$) rotational distributions from CF₃H, CH₃CF₃, and C₂F₅H. The highest observed rotational level and the fraction of the population in $J > 8$ decrease with increasing vibrational level. The emission from the $J > 8$ levels of the CH₃CH₂F reaction was too weak for a detailed analysis. The rotational distributions for the C₃F₇H reactions were 300 K, but these experiments were done for larger $P\Delta t$, for which rotational relaxation is more extensive and our observations do not preclude formation of some higher J levels.

In order to estimate the $\langle E_R(\text{HF}) \rangle$, the relative population in levels $J \geq 12$ were fitted to a Boltzmann distribution for reactions 1, 3, and 4 (Figure 5). The best-fit temperatures for $v = 1$ are 3100, 2625, and 2470 K for CF₃H, CF₃CH₃, and C₂F₅H, respectively. If these temperatures are associated with the nascent rotational distributions, we can obtain a lower limit to the rotational energy in HF($v=1$). Similar assignments were made for v

TABLE VI: Rotational Energy Disposal to HF^c

reagent	v	T_R	$\langle E_R \rangle$	$\langle g_R \rangle$	$\langle f_R \rangle^a$
CF ₃ H	1	3100	6.2	0.150	0.133 (0.125) ^b
	2	2670	5.3	0.170	
CF ₃ CH ₃	1	2625	5.2	0.077	0.055 (0.059) ^b
	2	2250	4.5	0.079	
CF ₃ CF ₂ H	1	2470	4.9	0.077	0.082 (0.059) ^b

^a Estimated by assuming that $\langle g_R \rangle$ for $v = 0$ and higher v levels were the same as those listed in the table; $\langle g_R \rangle = \langle E_R \rangle / (\langle E \rangle - E_v)$.

^b Calculated for the prior. ^c The $\langle f_R \rangle$ for CH₃CH₂F is much smaller than for CF₃CH₃; see text.

= 2 from the CF₃H and CF₃CH₃ reactions, and a summary of these analyses is given in Table VI. Next, the fraction of rotation energy relative to the total energy minus the HF(v) vibrational energy, $\langle g_R \rangle$, was calculated. The $\langle g_R \rangle$ values for $v = 1$ and $v = 2$ are nearly constant for both CF₃H and CF₃CH₃. If we assume $\langle g_R \rangle$ to be constant for all v levels of a given reaction (including $v = 0$), the total rotational energy can be estimated. This estimate of $\langle f_R \rangle$ is nearly equal to the value for the prior distribution for CF₃H and CF₃CH₃ as implied by the match for the distributions for $J \geq 12$ in Figure 4. For C₂F₅H only the $v = 1$ rotational distribution for C₂F₅H was analyzed because the emission intensity from higher v levels was too low. If we use this $\langle g_R \rangle$ for all v levels, $\langle f_R \rangle$ is estimated to be 0.08. The estimated $\langle E_R \rangle$ for CH₃CF₃ and C₂F₅H are similar because of the high weight given to $v = 0$ for the latter. The $\langle f_R \rangle$ appears to be larger for C₂F₅H because $\langle E \rangle - E_0$ is smaller. As already noted, the high- J component from the CH₃CH₂F reaction was too small to measure. Quick and Wittig⁷ estimated a HF rotational temperature of 800 K for C₂H₅F, which corresponds to only 4% above $J = 8$. The $\langle E_R(\text{HF}) \rangle$ from C₂H₅F is definitely less than for CF₃CH₃ or C₂F₅H, and the rotational energy disposal does change from one reaction to another.

We carried out a series of experiments with CF₃H for which the Ar pressure was increased at constant observation time (0.2 ms) from 0.4 to 1 Torr to increase the rotational relaxation. The fraction with $J > 8$ decreased with increase in Ar pressure. A linear extrapolation of the fraction with $J \geq 8$ to zero Ar pressure gave good agreement with the corresponding fraction for a 3100 K Boltzmann distribution, which has about 42% of the population in $J > 8$. Another point of view can be obtained by comparing the prior distribution to the experimental distribution; see Figure 4. The envelopes of the high- J components resemble the prior distributions. Recently Dietrich, Quack, and Seyfang³³ reported the time-resolved IRMPD of CF₂Cl-CH₂Cl; they noted that the nascent population in the $J = 0$ states of HCl($v=0, 1$) was essentially zero from time-resolved laser-diode spectroscopy. This observation supports our claim that the nascent distributions (for $v = 1$) have negligible populations in $J = 0-2$.

Discussions

1. Separating the Energy Disposal from the Excess Energy E_X and the Potential Energy E_P . Our results together with the efforts of previous investigators provide an experimental base for discussing three- and four-centered HX elimination reactions; two broad conclusions emerge about the HX product energy. Although the HX(v) distributions monotonically decline with v , the $\langle E_v(\text{HX}) \rangle$ is higher than expected statistically. On the other hand, the rotational excitation of HX is modest and fortuitously close to or less than the statistical expectation. Holmes and Setser¹³ accounted for the difference between the statistical predictions and the observed energy distribution by assuming that the E_X is statistically distributed at the transition state configuration but that E_P is released according to the local forces arising from the potential energy surface. ZL expressed this in a more quantitative way and defined the energy in HX vibration by the sum rule

$$\langle E_v(\text{HX}) \rangle = a\langle E_X \rangle + b\langle E_P \rangle \quad (13)$$

(33) Dietrich, P.; Quack, M.; Seyfang, G. *Chem. Phys. Lett.* **1990**, *167*, 535.

TABLE VII: Contributions from E_X and E_P to HF(ν)^a

reagent	$\langle E_V \rangle$	$\langle f_V \rangle$	$\langle E_V^{TS} \rangle$	a	$\langle E_P^T \rangle$	b
CF ₃ H	8.50	0.162	3.15	0.084	5.35	0.361
CF ₂ HCl	8.03	0.120	5.95	0.101	2.08	0.260
CFH ₂ Cl	7.12	0.153	4.23	0.110	2.89	0.340
CFHCl ₂	9.96	0.142	5.94	0.099	4.02	0.451
CF ₃ CH ₃	10.37	0.130	1.45	0.035	8.92	0.240
CH ₃ CH ₂ F	13.47	0.148	1.92	0.046	11.55	0.236
C ₂ F ₅ H	4.31	0.064	1.11	0.029	3.20 ^b	0.112

^a Energies in kcal mol⁻¹. ^b This small value probably is a consequence of both three- and four-centered elimination. The E_P associated with CF₃CF + HF formation would be quite small, even if b is of the same magnitude as for the CF₃H reaction ($\langle E_P^T \rangle$) would still be small.

Estimates of a were found from reactions without a barrier in the exit channel or by using statistical calculations; b was usually higher than a . All the reactions discussed in this paper have exit channel barriers, but a can be estimated from the statistical energy, $\langle E_V^{TS} \rangle$, in the coordinate associated with the HX vibrational motion at the transition state. Comparing this with E_X gives the value of a . This analysis, of course, assumes that HX stretching is separable from other motions at the transition state. Since $\langle E_V \rangle$ was determined experimentally, subtracting $\langle E_V^{TS} \rangle$ gives the HX vibrational energy obtained from the potential, $\langle E_P^T \rangle$, and comparison to E_P gives the value of b .

The transition-state parameters were taken from the literature for CF₃H,³⁴ C₂F₅H,^{30a} CH₃CH₂F,¹ and CF₃CH₃.³ The HF frequencies are ~ 1500 and ~ 1800 cm⁻¹ for the three- and four-centered transition states, respectively. Changing these frequencies by a few 100 cm⁻¹ does not alter $\langle E_V^{TS} \rangle$ significantly; however, lowering the frequency does slightly increase the vibrational energy because the heat capacities for the vibrational frequencies of the transition states are not at the classical limit for these values of E_X . The transition-state parameters are available for CFHCl₂³⁴ and CF₂HCl,²⁶ and the HCl stretching frequency was chosen to be 1050 cm⁻¹. The transition-state parameters for CFH₂Cl were chosen by comparison to these two molecules.

Table VII gives the a and b constants for reactions 1–4, 11, and 12. The calculations for C₂F₅H are based exclusively on a four-centered model. The three-centered reactions have $a \approx 0.1$ and $b \approx 0.3$ –0.4. The a values for C₂H₅F and CF₃CH₃ are smaller than for CF₃H because of the larger number of degrees of freedom. Both C₂H₅F and CF₃CH₃ have $b = 0.24$. For C₂H₅F and CF₃CH₃, which have approximately equal amounts of E_X and E_P , nearly all the HF vibration energy is obtained from E_P . Clearly, a significant fraction of E_P , $\sim 35\%$ for three-centered and $\sim 24\%$ for four-centered reactions, is converted into HX vibrational energy. The result from C₂F₅H differs from CF₃CH₃ and C₂H₅F; the low b value is further support that both three- and four-centered elimination occurs. If the C₂F₅H results were added to Table VII, their b values also would be low, which suggests that three-centered elimination may be occurring too. The results summarized in Table VII are combined with other data in the literature to obtain an overall view of three- and four-centered HX elimination in the following sections.

a. Three-Centered Reactions. Sudbo et al.¹⁰ measured the translational energy ($\langle E_T \rangle = 8.0$ kcal mol⁻¹) from IRMPD of CF₂HCl in a beam experiment. From the calculated RRKM rate constants and the laser pumping rate, E_X was estimated as ~ 7 kcal mol⁻¹. The barrier for the reverse reaction was taken as 6 kcal mol⁻¹; however, more recent classical studies^{23,26} suggest that the barrier is 8 kcal mol⁻¹. The higher value would be consistent with the experimental $\langle E_T \rangle$, which mainly arises from E_P . For a revised available energy of 15 kcal mol⁻¹, $\langle f_T \rangle$ would be 0.53. Stephenson and King (SK)¹¹ measured the complete energy distribution of CF₂ from CF₂HCl. Assuming a δ function for the velocity distribution for CF₂ gave good agreement with $\langle E_T \rangle$ from Sudbo et al.¹⁰ They found the rotational energy (6.0 kcal mol⁻¹) of CF₂ to be higher than the vibrational energy (3.6 kcal mol⁻¹). The total energy in the SK experiment presumably is similar to

the beam work. Combining all the results, including ~ 4 kcal mol⁻¹ for $\langle f_V(\text{HCl}) \rangle$, gives a total product energy of 21–22 kcal mol⁻¹, which obviously exceeds the estimated available energy. Either some of the data are in error or E_P is larger than 8 kcal mol⁻¹.

The $\langle f_V(\text{HCl}) \rangle$ and $\langle f_V(\text{HF}) \rangle$ from CFH₂Cl, CFHCl₂, and CF₃H resemble that for CF₂HCl, and Sudbo et al. also concluded that the translational energy disposal from CFHCl₂ was similar to that for CF₂HCl. We expect the dynamics from three-center elimination to be similar for all these reactions. In a contrary opinion, Samsonov and Petrov¹² claimed that the CHF resulting from IRMPD of CFH₂Cl was vibrationally very hot by measuring the rate constant of the unimolecular reaction of fluorocyclopropane formed from CHF + ethylene. But, the uncertainty in thermochemistry of the carbene and fluoro compounds, which forms the basis of their conclusion, is rather high.

In summary, the release of E_P from three-center HX elimination is as follows; $\langle f_T \rangle = 0.6$ and $\langle f_V(\text{HX}) \rangle = 0.3$ with the remainder released mainly to HX and carbene rotational energy. The vibrational energy of the carbene seems to be just the statistical component of E_X . More detailed interpretation is hampered by lack of reliable values for E_P for several of these reactions. The dominant aspect of the exit channel dynamics is the repulsive release of energy to translational motion, as mentioned by Sudbo et al.¹⁰ This general pattern also has been observed for the energy disposal to HF and CO in the elimination from HFCO activated by the F + HCO reaction,^{9b,c} although very careful control of the initially prepared state of HFCO by SEP experiments³⁵ may refine this point of view. Similar vibrational energy disposal patterns also have been found from HF elimination from HNF₂,³⁶ HSF₃,³⁷ and HSF,^{15a} although the rotational energy release for the latter was larger than for the halomethane reactions in Table VI.

b. Four-Centered Reactions. About 24% of E_P was released as $\langle E_V(\text{HF}) \rangle$ from CF₃CH₃ and CH₃CH₂F. The $\langle E_R(\text{HF}) \rangle$ from CF₃CH₃ is fortuitously close to the statistical limit (based on $E_X + E_P$), which means that about 12% of E_P is released as $\langle E_R(\text{HF}) \rangle$. But, $\langle E_R(\text{HF}) \rangle$ is much lower for C₂H₅F. Sudbo et al. found that about 20% of E_P was released as $\langle E_T \rangle$ from CH₃CCl₃. Thus, $\sim 45\%$ of E_P must remain as internal energy of the olefin for these haloethanes. This fraction of E_P plus the olefin's statistical share of E_X amounts to roughly 47 and 55 kcal mol⁻¹ for the CF₃CH₃ and CH₃CH₂F reactions, respectively. This energy is in accord with experiments³⁸ with CH₂ClCHCl₂ in which the 1,2-dichloroethene product did not have enough energy to undergo cis-trans isomerism, which has a 56 kcal mol⁻¹ threshold energy.

The division of E_P among the internal energy of the olefin, the relative translational energy, and the internal energy of HF is likely to show some variation from case to case, reflecting subtle features of the potentials.² In fact, the rather different $\langle f_R(\text{HF}) \rangle$ for CF₃CH₃ (~ 0.06) vs CH₃CH₂F (~ 0.02) serves to illustrate this point. Although the internal energy distribution was very broad, the mean fraction of E_P (0.32) received by methylcyclobutene^{13b} in the HCl elimination of methylchlorocyclobutane is less than the implied result for CF₃CH₃ or C₂H₅F. Since the carbon frame in cyclobutane is rather rigid, perhaps less potential energy is released to cyclobutene and more to translation energy than for the CF₃CH₃ and C₂H₅F reactions. Another interesting case⁸ is HF elimination from CH₂CFCl activated by photoabsorption at 193 nm; E_X is 68 kcal mol⁻¹ and E_P is ~ 63 kcal mol⁻¹. The $\langle f_V(\text{HF}) \rangle$ is 0.15 with a distribution similar to that from CF₃CH₃ and C₂H₅F, and in fact, the b constant calculated from their distribution also is similar. The HF rotational energy appears to be high, but the available energy of the reaction is very large, and the estimated mean HF rotational energy is not so different from the statistical expectation (as we have found for CF₃CH₃). The $\langle f_T \rangle$ from photolysis of an analogous molecule, CH₂CCl₂, was only ~ 0.1 (or 0.15 of the E_P), which suggests that $\geq 45\%$ of E_P goes to the internal energy of the HC₂Cl product.³⁹ Thus,

(35) Choi, Y. S.; Moore, C. B. *J. Chem. Phys.* **1990**, *90*, 3875; Abstract 71 of the Physical Division, 199th ACS Meeting, April 22–27, 1990.

(36) Malins, R. J.; Setser, D. W. *J. Phys. Chem.* **1981**, *85*, 1342.

(37) Malins, R. J.; Setser, D. W. *J. Chem. Phys.* **1980**, *73*, 5666.

(38) Kim, K. C.; Setser, D. W. *J. Phys. Chem.* **1974**, *78*, 2166.

(34) Chang, H. W. Ph.D. Thesis, Kansas State University, 1971.

there seem to be examples for which either less or more energy is released to the olefin than the 45% expectation based upon data for CF_3CH_3 and $\text{C}_2\text{H}_5\text{F}$. The major difference between the energy disposal of the four-centered elimination reactions and those three-centered processes with significant E_p is the time scale for release of the energy associated with the relaxation associated with formation of the C–C double bond, which occurs after the H has migrated to the X atom but during the departure of FH from the olefin.

2. The $\text{HF}(v)$ Distribution from Release of E_p . Since the majority of the HX vibrational energy arises from E_p , it is desirable to extract the $\text{HX}(v)$ distribution associated with the release of E_p from the overall experimental distribution, i.e., what would be the observed $\text{HF}(v)$ distribution for molecules with $E_X \approx 0$. We will take the simplest point of view and assume that each of the insipient $\text{HF}(v)^\ddagger$ states leaving the transition-state configuration acquires the same average vibrational energy in traversing the exit channel where E_p is released. That is, the release of E_p to HF is not dependent on "starting" conditions from the transition state. As will be demonstrated, the distribution associated with E_p can be characterized by a Boltzmann temperature, which is chosen such that when combined with the $\text{HF}(v)^\ddagger$ distribution leaving the transition state the experimental $\langle E_v(\text{HF}) \rangle$ and distribution is matched. Stated another way, these Boltzmann temperatures represent the distributions that can be associated with the b values of Table VII.

The nominal HF stretching frequency needed to describe the Boltzmann distribution for the release of E_p must be sufficiently small that the partitioning of E_p can be reliably modeled (i.e., the Boltzmann distribution must be sufficiently fine grained). For example, the barrier energy is only 15.8 kcal mol⁻¹ for CF_3H , and using the true HF frequency 4138 cm⁻¹ (11.8 kcal mol⁻¹) would not be adequate. For convenience in representing the Boltzmann distributor, we utilized the HF^\ddagger frequency of the transition-state configuration. Since these frequencies are roughly half of the true HF frequency, there are approximately 2 times as many levels in the calculated final product distribution as in the HF distribution. The populations in the intermediate levels were distributed to neighboring levels in a way to maintain the overall integrity of the final calculated distribution. The criterion used for requantizing the $\text{HF}(v)$ distribution was that the energy associated with each nominal level was conserved in the redistribution process. This situation is somewhat analogous to classical trajectory calculations, where the calculated product vibrational energy is quantized by assuming that trajectories with energy of $(n - 1/2)h\nu$ to $(n + 1/2)h\nu$ correspond to the state n . The selection of a Boltzmann type distribution for partitioning E_p was the first choice, and it proved satisfactory. However, a linear surprisal type distribution for the release of E_p would work equally well.

The temperatures that were required to fit the CF_3H , CF_3CH_3 , and $\text{CH}_3\text{CH}_2\text{F}$ distributions were 6200, 6680, and 8185 K, respectively. Figure 6 compares the observed and calculated $\text{HF}(v)$ distribution for CF_3CH_3 reaction; the agreement is acceptable. The agreement between calculated and observed results also was satisfactory for $\text{CF}_3\text{CF}_2\text{H}$ ($T = 2770$ K); the much lower temperature reflects the difference in $\langle f_v(\text{HF}) \rangle$ between $\text{CF}_3\text{CF}_2\text{H}$ and CF_3CH_3 (or $\text{C}_2\text{H}_5\text{F}$). No calculations were done for the HCl reactions, since the E_p values are small (and very uncertain).

Conclusions

We have studied the HF and HCl vibrational and rotational energy disposal from the three-centered unimolecular elimination reactions of chloro- and fluoromethanes and the four-centered reactions of fluoroethanes. The molecules were formed with ~ 105 kcal mol⁻¹ of energy by atom + radical recombination reactions. Each reaction has a sizable potential barrier for the reverse reaction. The HF and HCl vibrational distributions from both three-

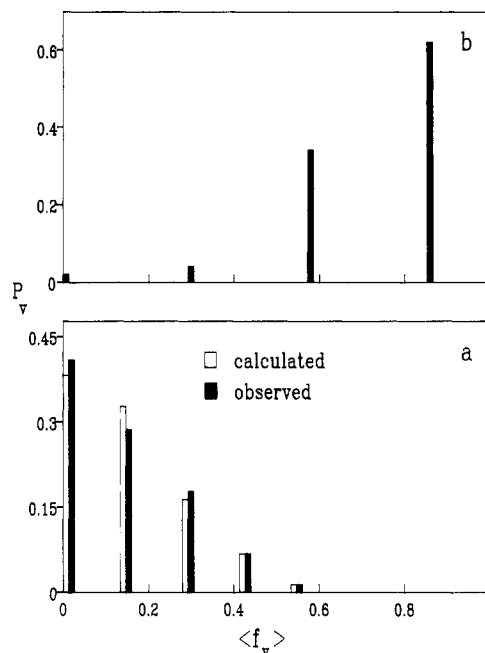


Figure 6. (a) Comparison of the $\text{HF}(v)$ experimental and calculated vibrational distributions for the CF_3CH_3 reaction. The calculated distributions represent the convolution of the statistical distribution at the transition state plus a Boltzmann type distribution associated with release of E_p ; see text. (b) Typical $\text{HF}(v)$ distribution from a C–H abstraction reaction; the data are for $\text{F} + \text{CH}_2\text{ClF}$. Similar distributions are found for F atom reactions with other methyl halides.^{15c}

and four-centered elimination reactions contrast strongly with hydrogen abstraction reactions; see Figure 6. For hydrogen abstraction reactions, $\langle f_v(\text{HF}) \rangle$ is about 0.6, the vibrational distributions are highly inverted, and they extend to the thermochemical limit.^{15c} Elimination reactions, on the other hand, have $\langle f_v \rangle$ of only 0.1–0.2 with monotonically declining distributions. We also studied the $n\text{-C}_3\text{F}_7\text{H}$ and $i\text{-C}_3\text{F}_7\text{H}$ reactions; the smaller $\langle f_v(\text{HF}) \rangle$ was interpreted as evidence for competing three- and four-centered elimination. A similar competition probably occurs for $\text{C}_2\text{F}_5\text{H}$.

The excess energy above the threshold energy, approximately 40–50 kcal mol⁻¹, is statistically distributed at the transition-state geometry. About 10% of the E_X will contribute to HCl or HF vibrational energy for the three-centered elimination from the halomethanes; this statistical component decreases to 5% of E_X for the four-centered reactions of the fluoroethanes. The potential energy of the exit channel is preferentially released as HX vibrational energy for both three- and four-centered reactions. For the three-centered cases approximately 35% of the rather small E_p goes to $\langle E_v(\text{HF}) \rangle$, whereas 24% of E_p goes to $\langle E_v(\text{HF}) \rangle$ for the four-centered reactions. Deconvolution of the statistical component from the total $\text{HF}(v)$ vibrational distributions suggests that the HF vibrational distribution associated with the release of E_p is Boltzmann-like. Estimates for $\langle E_R(\text{HF}) \rangle$ indicated that the rotational energy is always less than $\langle E_v(\text{HF}) \rangle$, but $\langle f_R(\text{HX}) \rangle$ probably changes more from one reaction to another than does the $\langle f_v(\text{HX}) \rangle$. The $\langle f_R(\text{HF}) \rangle$ for CF_3H , CF_3CH_3 , $\text{C}_2\text{F}_5\text{H}$, and $\text{C}_2\text{H}_5\text{F}$ were estimated as 0.13, 0.06, 0.08, and ~ 0.02 , respectively. According to data in the literature for the haloethanes, about 20% of E_p is released as relative translational energy and, by difference, about 45% of E_p is released as internal energy of the olefin. The three-centered reactions release a larger fraction of the energy to relative translation and a smaller proportion to the carbene.

Our data can be directly compared to recent theoretical treatments of four-centered elimination reactions.^{2,3} Raff and Graham were able to do classical trajectory calculations to describe the full dynamical history of the $\text{CH}_2\text{FCH}_2\text{F}$ reaction with internal energies of 138–207 kcal mol⁻¹. Their model showed the expected statistical behavior regarding the dependence of the unimolecular decay lifetimes vs energy. The trajectory calculation gave $\langle f_v$

(39) Umenoto, M.; Seki, K.; Shinohara, H.; Nagashima, U.; Nishi, H.; Kinoshita, M.; Shimada, R. *J. Chem. Phys.* **1985**, *83*, 1657.

(40) Palsey, S. D.; Holmes, B. E. *J. Phys. Chem.* **1983**, *87*, 3043. This work proves that HX elimination is a syn process; i.e., the hydrogen and halogen are removed from the same side of the parent molecule.

(HF)) in the range 0.08–0.09, which is somewhat lower than our experimental results for C_2H_5F and CH_3CF_3 . The large E_X used for the calculations, however, tends to reduce $\langle f_V(HF) \rangle$ because the statistical contributions to $\langle E_V(HF) \rangle$ from E_X is small. In fact, using the a and b constants of Table VII with the E_X and E_P for the calculation by Raff and Graham gives a $\langle E_V(HF) \rangle$ that is not far from their computed $\langle f_V(HF) \rangle$. Nevertheless, the calculated vibrational distribution seems too narrow and $\langle E_V(HF) \rangle$ probably is slightly low. The calculated $\langle f_R(HF) \rangle$ was about 1/2 of $\langle f_V(HF) \rangle$, which matches the experimental trend. The informative plots of the R_{H-F} , R_{C-F} , and R_{C-H} distances vs time for HF elimination given by Raff and Graham explicitly confirm the intuitive view of Setser and Holmes^{13b,c} that these reactions proceed by migration of H to the halogen atom followed later by rupture of the carbon–halogen bond and movement of the XH away from the olefin. The trajectory calculations show that this time delay is $\geq 7 \times 10^{-14}$ s. The HF amplitude of vibration following migration of the H *never* indicates the receipt of a large amount of energy by HF; i.e., internal energy is not deposited in HF and then subsequently removed via an internal coupling. The dynamics associated with the C–F bond rupture and the changes in the internal coordinates within the olefin are not so well understood. Kato and Morokuma tried to analyze these changes using their *ab initio* potential surface for C_2H_5F and identified the major coordinates associated with the release of energy, but they did not do any trajectory calculations. Benito and Santamario² carried out classical trajectory calculations on five different empirical potential surfaces for the CF_3CH_3 reaction. These surfaces were

adjusted in an attempt to correlate the energy disposal with the important features of the exit channel potential. They started the trajectories at the transition-state geometry for particular assignments of E_X in order to reduce the time required for the calculation. This was necessary because they used a more modest total energy than did Raff and Graham. All five surfaces seem to match the general pattern for energy disposal by four-centered processes, but $\langle f_T \rangle$ seems too small for all choices. Surface 3 with 12%, 19%, 1%, and 60% for the fraction of E_P released to E_T , $E_V(HF)$, $E_R(HF)$, and $E_V(CH_2CF_2)$, respectively, seems best to match the experimental result (20%, 20%, 10%, and 50%, respectively). Increasing the *asymmetry* and *steepness* of the release of the potential energy as HF and $C_2F_2H_2$ separate, which should augment $E_R(HF)$ and E_T , respectively, would improve the match with the experimental results. The combination of better experimental data and further exploration of the potential surfaces will improve our understanding of the many-body effects in these elimination reactions. The complex energy release pattern for the four-centered HX elimination reactions is consistent with the inability to drive the reverse, addition reactions by placing vibrational energy in only the HX or only the olefin reactant.⁴¹

Acknowledgment. This work was supported by the National Science Foundation (Grant 86-01599). We thank Mr. Srinivas Jampani for assistance with some of the experiments.

(41) (a) Herman, J. P.; Marling, J. B. *J. Chem. Phys.* **1979**, *71*, 643. (b) Klenerman, D.; Zare, R. N. *Chem. Phys. Lett.* **1986**, *130*, 190.

Ferrocene Molecular Reorientation in the (Thiourea)₃·Ferrocene Inclusion Compound As Studied by ²H NMR Spectroscopy

Stephen J. Heyes, Nigel J. Clayden, and Christopher M. Dobson*

Inorganic Chemistry Laboratory, University of Oxford, South Parks Road, Oxford, OX1 3QR, U.K.
(Received: June 27, 1990)

The molecular reorientational dynamics of ferrocene included in the (thiourea)₃·ferrocene complex have been studied by ¹³C CP/MAS NMR and ²H NMR spectroscopy. Analysis of the ²H NMR line shapes has allowed delineation of two distinct reorientational processes among the four distinguishable orientations of ferrocene suggested to be populated in this inclusion compound. Kinetic parameters have been estimated as $E_a = 6.4 \pm 0.5$ kJ mol⁻¹ with $A = (2.15 \pm 0.5) \times 10^7$ s⁻¹ for the direct interchange between the three orientations perpendicular to the host channel axis, and $E_a = 10.1 \pm 1.0$ kJ mol⁻¹ with $A = (1.5 \pm 0.6) \times 10^8$ s⁻¹ for parallel–perpendicular orientational interchange. These results are compared with rates found from ⁵⁷Me Mössbauer studies and ¹³C NMR spectra of powder and oriented samples.

Introduction

We have developed a strategy of using the ²H NMR spectroscopy of perdeuterated metallocene probe molecules to explore the molecular reorientational dynamics of guest metallocene molecules in a wide variety of solid-state environments.^{1–4} The knowledge of the possibilities for guest molecule dynamics reveals

features of interest concerning the structure of inclusion and intercalation compounds, and the nature of the host–guest interaction. Here we examine the application of this approach to the area of clathration by thiourea.

Thiourea forms channel type inclusions with a variety of guest molecules including branched-chain alkanes, fatty acids, and cycloalkanes. Previous crystallographic, wide-line NMR, and thermal studies in many of these clathrates suggest that the guest molecules are loosely held by the host lattice, allowing considerable degrees of molecular motion.⁵ Clement et al.⁶ found that it was

(1) Clayden, N. J.; Dobson, C. M.; Heyes, S. J.; Wiseman, P. J. *J. Inclusion Phenom.* **1987**, *5*, 65–68.

(2) Heyes, S. J.; Clayden, N. J.; Dobson, C. M.; Green, M. L. H.; Wiseman, P. J. *J. Chem. Soc., Chem. Commun.* **1987**, 1560–1562.

(3) Heyes, S. J. D. Phil. Thesis, University of Oxford, 1989.

(4) Heyes, S. J.; Dobson, C. M. *Magn. Reson. Chem.* **1990**, *28*, S37–46.

(5) Takemoto, K.; Sonoda, N. In *Inclusion Compounds*; Atwood, J. L., Davies, J. E. D., MacNicol, D. D., Eds.; Academic Press: London, 1984; Vol. 2, pp 47–67.